Electroanalysis

WILEY VCH

ELECTROANALYSIS
An International Journal Devoted to Electroanalysis, Sensors and Bioelectronic Devices

RESEARCH ARTICLE OPEN ACCESS

Exploring High-Charge-Density Polyelectrolytes as Membrane Component for Solid Contact Ion-Selective Electrodes

Júlia Mestres[1,2] | Jayaruwan G. Gamaethiralalage[1] | Louis C. P. M. de Smet[1] | Francesca Leonardi[2]

[1]Laboratory of Organic Chemistry, Wageningen University, Wageningen, the Netherlands | [2]Stichting imec Nederland within OnePlanet Research Center, Wageningen, the Netherlands

Correspondence: Louis C. P. M. de Smet (louis.desmet@wur.nl) | Francesca Leonardi (francesca.leonardi@imec.nl)

Received: 10 April 2025 | **Revised:** 28 June 2025 | **Accepted:** 8 July 2025

Funding: Dutch Research Council, Grant/Award Number: ENPPS.LIFT.019.034; European Research Council, Grant/Award Number: 101158035; Provincie Gelderland

Keywords: hydrophilic polymeric membranes | ion-selective membrane | polyelectrolyte | potassium sensor | solid contact ion-selective electrodes

ABSTRACT

Polyanions have been introduced as replacements for poly(vinyl chloride) (PVC) and potassium tetrakis(4-chlorophenyl)borate (KTpClPB) in the preparation of solid contact potassium-ion selective electrodes (K^+-ISEs). Partly carboxylated PVC (PVC-COOH) and a fully charged polyanion, sodium poly(4-styrenesulfonate) (NaPSS), were used, culminating in the fabrication of three-component ion-selective membranes (ISMs). The comparison with a PVC-based ISM showed significantly reduced potential drifts during conditioning (from ~1.3 to ~0.2 mV/h) and a constant drift rate. Reduced drift is attributed to the presence of counter-charges in the polymer and the large molecular weight of the polyanions, therefore decreasing the leaching of the components resulting in degradation of the membrane. The ISEs utilizing the hydrophilic and highly charged NaPSS as the polymer matrix exhibit similar water layer formation compared to the PVC-based ISEs, and maintained a sensitivity of 54 ± 1 mV/dec and a selectivity over sodium of −3.1 (log $K^{pot}_{K^+, Na^+}$) after 1 week in solution, suggesting an alternative approach to the standard membrane preparation protocol.

1 | Introduction

The fabrication of wearable and portable potentiometric ion-sensing devices has gained significant popularity with various applications [1], ranging healthcare diagnostic [2, 3], agricultural monitoring [4], sensing devices with forensics or pharmaceutical purposes [5], and water contaminant detection [6, 7]. Among the various sensing strategies available, all-solid-state, ion-selective electrodes (ISEs)–also called solid contact (SC) ISEs–have the advantage of being miniaturized and stored under dry conditions, requiring less sample volume and maintenance [8].

A key functionality of SC-ISEs is their affinity layer, named ion-selective membrane (ISM), which is set to make the sensor selective toward a specific analyte. Such a layer is often prepared by mixing four different components, i.e. i) an ionophore, a.k.a. the ion receptor, ii) a lipophilic salt that acts as an ion buffer/exchanger, iii) a polymeric matrix such as poly(vinyl chloride) (PVC) as a flexible, structural support, and iv) a plasticizer to support dissolution of the other components and enhance flexibility of the membrane by decreasing the glass transition temperature of PVC [8, 9]. The lipophilic salt acts as a counter-charge to the primary ion of interest and imposes a permselective effect, called the Donnan exclusion effect [8, 10, 11]. Furthermore, it provides additional ionic sites, reducing the resistance of the membrane [9, 12]. For plasticized-PVC potassium ISEs (K^+-ISEs), a borate lipophilic salt such as potassium tetrakis (4-chlorophenyl)borate (KTpClPB) is typically used as a negatively charged additive [12–14].

Preparing ISMs by mixing the four key ingredients is the most straightforward approach. However, a drift of the sensor response limits the use of ISEs for continuous monitoring due to the need of regular calibrations [1, 15]. Such a drift may be originated by the spontaneous leaching of low molecular weight (MW) membrane components, as well as the formation of a water layer between the SC and the ISM [16, 17]. Various solutions have been proposed to reduce leakage, such as covalently attaching some of the membrane components [18–20], or the use of high MW plasticizers [21]. Other approaches focused on immobilizing the membrane to the SC by employing porous materials or chemically bonding the ISM to the SC [22, 23]. The preparation of three-component ISE membranes with (plasticizer-free) elastomeric polymers, e.g. polysiloxanes, has also been explored [24, 25].

There is only a limited number of studies that have explored the use of charged polymers in the preparation of ISMs, and in most of these cases, modified PVC and a liquid-contact configuration were employed, with a strong focus on carboxyl and amine functional groups [26]. These low-charge-density polyelectrolytes (PEs), i.e. only a few percent of the monomers are charged, do not only improve the membrane adhesion on silicon substrates [27], but they increase biocompatibility [26, 28], and enable a large variety of functionalization schemes, including biomolecule immobilization [26]. Moreover, ionophore-free ISMs made with low-charge-density aminated PVC functions as a pH sensor [29]. Responses to H^+ and K^+ [30], as well as F^- [31], has also been observed for ion-exchanger-free ISMs made with low-charge-density PVC-COOH. Nevertheless, it remains good practice to add free lipophilic borate salt to reduce the membrane resistance [28, 32]. Lastly, next to carboxylation and amination, sulfonation of PVC has also been explored, albeit in the fields of cation-exchange resins [33] and proton-conductive membranes [34], rather than ISMs.

Rosatzin et al. compared several borate salts, including a sulfonated copolymer with immobilized ionic sites. Unfortunately, no functionalization degree is reported and the wt% is kept to the typical values of the lipophilic component [35]. One interesting PE is sodium poly (4-styrenesulfonate) (NaPSS), which in combination with poly (3,4-ethylenedioxythiophene) (PEDOT) or polypyrrole (PPy) forms a conductive material (e.g. PEDOT:PSS) often used for the preparation of SCs for SC-ISEs [36–39]. Furthermore, it can be combined with other materials such as graphene oxide (GO) for the fabrication of nanostructured ISMs, with the aim of mimicking selective nanochannels found in biological systems [40]. Some studies used NaPSS to build layer-by-layer (LbL) membranes, serving as transducer layers for the fabrication of K^+- and Na^+-ISEs [41, 42], although it is more common to find LbL in applications oriented to water purification [43] or in capacitive deionization (CDI) membranes [44, 45]. Bakker and coworkers employed ion-exchange membranes (based on PEs) for liquid contact ISE fabrication, obtaining good slopes but low selectivity compared to ionophore-based ISEs [46].

To the best of our knowledge, incorporation of high-charge-density PEs, for example one charge per monomer, in ISMs has not been explored. Therefore, in this work we explore the feasibility of utilizing polyanions to fabricate four- and three-component K^+-ISMs on solid-state ISEs. The polyanion replaces two of the traditional membrane components: the matrix materials (PVC) and the lipophilic salt (KTpClPB) (Figure 1A). ISEs prepared with low-charge-density PVC-COOH and high-charge-density NaPSS were compared. The ISMs have been characterized morphologically (wettability), and the ISEs electrochemical performance (selectivity, sensitivity, capacitance, and resistance) has been studied to elucidate their stability over time.

2 | Materials and Methods

2.1 | Reagents and Instruments

High-molecular-weight poly (vinyl chloride) (PVC, 90 000 g/mol, ~1440 monomers), bis (2-ethylhexyl) sebacate (DOS), potassium tetrakis (4-chlorophenyl)borate (KTpClPB), potassium ionophore I (valinomycin, (Figure S1)), potassium chloride (KCl), sodium

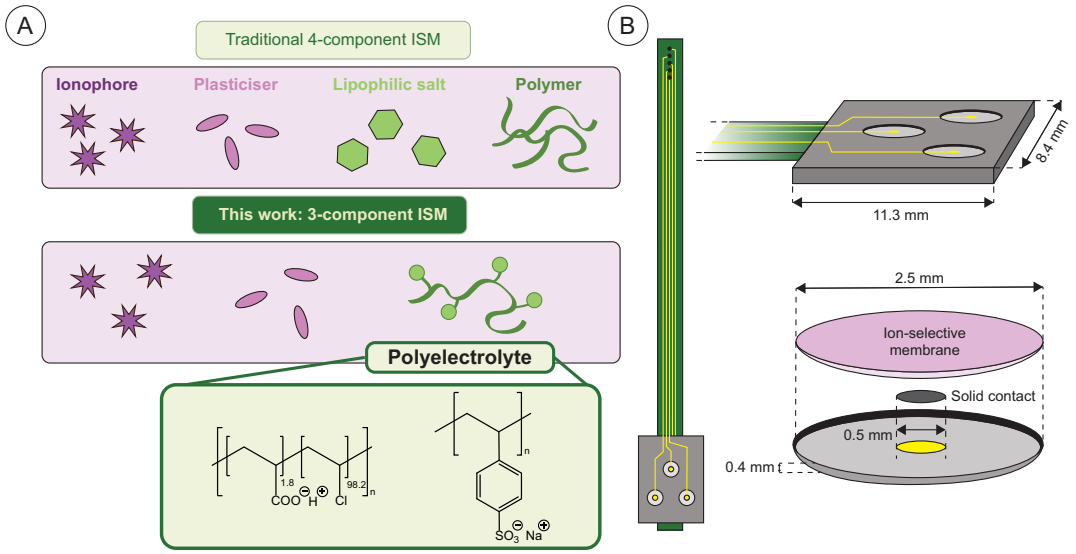

FIGURE 1 | (A) Overview of the strategy of employing high-charge-density PEs in K^+-ISMs. (B) Micrograph of the sensor substrate composed of three independent gold contacts of 0.5 mm diameter inside a glass reservoir of 0.4 mm thickness. The layers comprising the SC-ISE include the SC carbon ink that completely covers the gold surface, while the ISM is drop-cast to fill the hole reservoir.

chloride (NaCl), and cyclohexanone were purchased from Sigma–Aldrich (Selectophore grade). Poly(sodium 4-styrenesulfonate) (NaPSS, 70 000 g/mol, ∼340 monomers) were purchased from Sigma–Aldrich. Poly (vinyl chloride) carboxylated (PVC-COOH, 1.8 wt% carboxyl content, 220 000 g/mol, ∼55 carboxyl monomers, ∼3508 monomers in total) was purchased at Thermo Scientific Chemicals. No further purification was performed. A carbon conductive ink (Micromax BQ226) was employed as SC and used as received. All aqueous solutions employed for potentiometric experiments were prepared with ultrapure water (Milli-Q IQ 7000 purification system, resistivity ∼18.2 MΩ·cm). Membrane images were taken with a MikroCam II 3.2 MP camera (BRESSER) coupled to a KERN & Sohn GmbH OZL-963U microscope.

All three-electrode configuration experiments were performed using an Autolab (PGSTAT128N, Metrohm BV, The Netherlands) potentiostat/galvanostat with a double junction Ag/AgCl (3 M KCl bridge and electrolyte filling, type 6.0729.100, Metrohm) reference electrode and a Pt wire (IS-PT.W.CE, PalmSens) as the counter electrode. Ion chromatography showed no significant KCl leakage from the RE. All potentiometric measurements were performed using a high-input impedance (10^{12} Ω) meter (Jenco 6250 pH/mV/Ion meter).

2.2 | Fabrication of SC K^+-ISEs

The sensor substrate presented in this work was fabricated by Micronit (Enschede, Netherlands). A complementary metal–oxide–semiconductor-compatible production process was employed to pattern gold electrodes on Si/SiOx wafers (containing ∼100 sensors of ∼150 mm). Each chip comprises three gold contacts, which serve as working electrodes (WE, 0.5 mm diameter). The top surface was sealed with a glass cover (0.4 mm thick) possessing three apertures matching the three Au contacts. This structure ensured the presence of three reservoirs (2.5 mm in diameter, 0.4 mm in height) for the deposition of the membrane (Figure 1B), and it allowed the collection of triplicate measurements during each experiment.

To prepare the K^+-ISE, the gold substrate was first cleaned by electropolishing using 0.05 M H_2SO_4 (12 cycles from −1.0 to +1.0 V at 0.1 V/s scan rate). After electropolishing, the sensor was thoroughly rinsed with water and dried with compressed air. The conductive carbon ink was drop-cast on the gold substrate and cured for 15 min at 130°C. Once cooled down, the sensor was rinsed with water and dried in air.

Two sets of K^+-ISM have been prepared. Cyclohexanone was employed as membrane solvent aiming for better manipulation and reduced evaporation of the membrane stock solution [47–50]. Additionally, the higher polarity of cyclohexanone, compared to tetrahydrofuran, makes it a suitable solvent for the hydrophilic PEs added in the membrane.

The first set aimed to study the effect of replacing the lipophilic salt (KTpClPB) with one of the investigated PEs (PVC-COOH and NaPSS). All four-component membranes were prepared by dissolving 2.6% (w/w) valinomycin, 32% (w/w) PVC, and 65% (w/w) DOS, and a molar ratio of 2.2 for the ionophore with respect to the counter-charges (see Table S1). The mixture was then dissolved in 1 mL of cyclohexanone. Additionally, an ISM named "no salt" which lacks the lipophilic agent, was prepared as a blank membrane.

In the second set of K^+-ISMs, the investigated PEs replaced the polymeric matrix partially (25% or 50%) or fully (100%), where in the latter case the ISM consists of three components. For this set, all membranes maintained a 2.8% (w/w) valinomycin, 32% (w/w) polymer (i.e. PVC + PE or PE only), and 65% (w/w) DOS, dissolved in 1 mL of cyclohexanone. In this scenario, the ratio of ionophore to ionic sites is significantly lower than those of standard membrane compositions. As a control, NaPSS membranes without an ionophore were prepared to study whether NaPSS influences the selectivity coefficient (see Table S1).

The membrane mixture was deposited in the sensor reservoir using a 5 μL glass syringe. First, 2 μL of the membrane mixture was drop-cast and allowed to dry for 24 h at room temperature. Then, the process was repeated with an additional 1 μL aliquot of membrane cocktail to ensure a proper filling of the reservoir. The final membrane thickness was 21 ± 3 μm ($n = 13$), measured by a confocal sensor (MicroEpsilon confocalDT model IFS2405−0.3).

2.3 | Membrane Wetting and Mechanical Properties

Membrane wettability was determined by measuring the static water contact angle (SWCA) using a drop shape analyzer (Kruss; 3 μL water droplet volume; sessile drop method, ellipse (Tangent-1)), controlled by the ADVANCE software (version 1.8.0.4). The membranes were drop-cast (5 μL) onto a glass slide and let dry overnight. The measurements were done in triplicate, and each measurement recorded the SWCA value every second during the first 10 s after the water droplet deposition.

Some mechanical properties of the reference and 100% NaPSS membranes were studied. A semiquantitative adhesion test was performed by tearing up Scotch tape from the sensor chip (dry after use) [51, 52]. Additionally, the membrane solution was drop-cast (20 μL) on a glass slide and on the C-ink, to evaluate the adhesion on different substrates. The tape was gently pressed onto the ISM to ensure contact, and was quickly removed after 30 s. The viscosity of the two freshly stirred membrane mixtures was measured with an Anton Paar MCR 702e MultiDrive with a measuring bob DG26.7 at room temperature. Rheological properties were characterized in an Anton Paar RheoCompass MCR 501 rheometer with a 10 mm smooth flat parallel plate system. Parameters (yield stress and modulus of elasticity) were obtained performing an amplitude sweep (log strain ramp from 0.1 to 1000%), at a fixed normal force of 1 N, dry conditions, and room temperature.

2.4 | Galvanostatic Charge/Discharge

Current reversal chronopotentiometry (CRC)–also named constant-current chronopotentiometry or galvanostatic charge/discharge–was used to determine the electrode capacitance and resistance [17, 53, 54]. Measurements were done using a three-electrode configuration in a 10 mM KCl solution at room temperature. The sensor was polarized by applying a small direct

current of 10 nA for 60 s (charge step), then switched to–10 nA (discharge step) for another 60 s. This charge–discharge process was repeated three times, and each membrane was measured in triplicate, after 1 and 7 days. The electrode capacitance (C) was calculated as $I \times \Delta t/\Delta E$, where I is the current applied and $\Delta t/\Delta E$ the slope of the linear section of the discharge curve. The resistance (R) was calculated as $\Delta E_{switch}/I$, where ΔE_{switch} is the potential jump when switching the current from positive to negative. Using this method, the measured C corresponds to the overall interfacial capacitance.

2.5 | Potentiometric Measurements

Open-circuit potential (OCP) measurements were conducted in a two-electrode configuration, by measuring the K^+-ISE versus a double junction Ag/AgCl reference electrode. The sensors were calibrated by measuring the K^+ concentration in the range of 10^{-7} to 10^{-1} M KCl, in Milli-Q ultrapure water or background electrolyte of 0.1 M NaCl (all solutions with a pH value between 5.5 and 6.1). The OCP at each concentration step was recorded for 5 min and averaged. The linear range of the calibration curve was used to calculate the slope and offset (E^0) was from 10^{-4} to 10^{-1} M. At least five replicates were measured per ISM, and a box plot analysis was used to identify outliers [55]. Standard deviations are influenced by the inter-batch variability, unavoidable due to the manual drop-casting method of the SC and the ISM.

The selectivity was determined by calculating the selectivity coefficient ($K^{pot}_{K^+, Na^+}$) using the fixed interference method (FIM) [8]. This method consists of varying the concentration of the primary ion (a_A) while keeping a constant background of the interfering ion (a_B). In Equation (1), z_A and z_B have the same signs and a_A is obtained by determining the intersection of the extrapolation of the linear portions of the calibration curve [56].

$$K^{pot}_{A,B} = a_A/(a_B)^{z_A/z_B} \quad (1)$$

Finally, a water layer test was performed to evaluate the accumulation of water at the interface between the carbon ink and the ISM. The test consisted of a first equilibration step of the sensor in a 10 mM KCl solution for 1 h, followed by 10 mM NaCl for 2 h, before moving back to 10 mM KCl for 3 h. Electromotive force (EMF) values in the primary ion solution were evaluated as an indication of water layer formation [53].

3 | Results and Discussion

3.1 | Membrane Hydrophobicity, Capacitance, and Resistance

SWCA data (Figure 2A) reveal a slightly hydrophobic surface of the reference membrane composition (85°) [57, 58]. By replacing KTpClPB with PEs (first set), the SWCA values remain high,

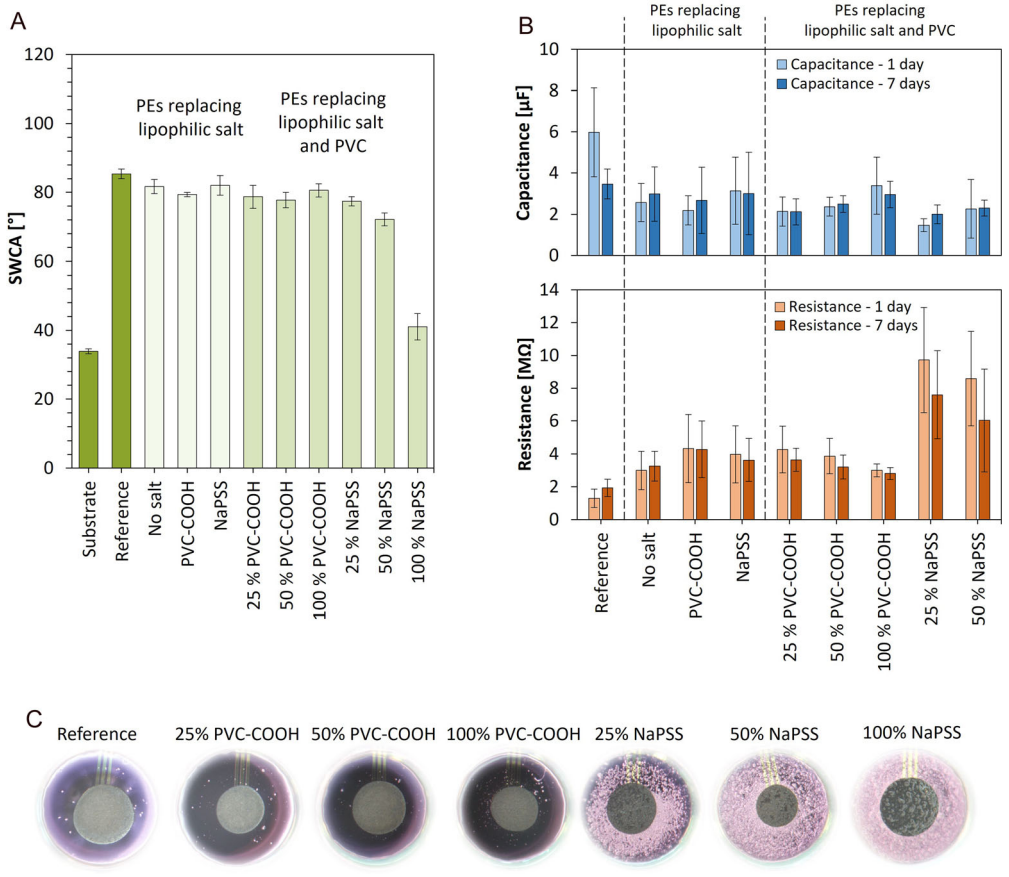

FIGURE 2 | (A) SWCA data of K^+-ISMs drop-cast on a glass substrate. The error bars correspond to the standard deviation of three replicates. (B) Capacitance and resistance of the K^+-ISMs after 1 day (light color) and 7 days (dark color) in 10 mM KCl, measured by CRC. The error bars correspond to the standard deviation of a minimum of three replicates. (C) Pictures of the second set of K^+-ISM before use.

between 79° and 82°. This can be rationalized as the relative amount of PE is as low as 0.2 wt% (see Table S1) and the polymer matrix and the plasticizer largely dominate the overall membrane surface wettability.

In the second set of ISMs, no lipophilic salt was used, and the PVC content (32 wt%) was gradually reduced by introducing a polyanion until a PVC-free, three-component membrane was obtained. Wettability values for the PVC-COOH membrane compositions are in line with the reference recipe, obtaining SWCA values of 79° (25% PVC-COOH), 78° (50% PVC-COOH), and 81° (100% PVC-COOH). Despite the significantly increasing addition of PVC-COOH, the small difference in SWCA data can be rationalized by the low carboxyl fraction of PVC-COOH (1.8 wt%). Additionally, protonation of all carboxylated groups is not guaranteed, and as a consequence, the bulk behavior is similar to the one of PVC-ISM [29, 30].

In contrast, increasing NaPSS concentrations from 25% to 50% and eventually 100% results in SWCA values decreasing to 77°, 74°, and 41°, respectively. The similar SWCA values for the 25% and 50% formulations to the contact angle of the reference composition (85°) indicate that the interfacial properties are comparable and therefore, dominated by the PVC. The distribution of the membrane components across the membrane is known not to be homogeneous, as reported by previous research showing that the lipophilic plasticizer predominates at the surface [59]. In our scenario, due to the hydrophilic nature of NaPSS, miscibility with other membrane components is reduced, a phenomenon manifested during and after the membrane preparation (see Figure 2C). All compounds can be stirred homogeneously during the membrane preparation, but after the deposition by drop-casting, the membrane formation process becomes uncontrolled, leading to phase separations [9]. Due to the higher affinity of hydrophobic compounds with air [60], PVC may move toward the surface, resulting in a similar SWCA. When no PVC is added (100% NaPSS), this is no longer observed, as reflected by the drop in the SWCA.

Next, we mapped and compared the bulk electrochemical characteristics of the ISMs by employing CRC as described in Section 2.4. Figure S2 illustrates the nonlinear chronopotentiometric curves characteristic of ISMs [61–63]. Following the conditioning step (membrane hydration), the reference membrane prepared with KTpClPB exhibits the highest capacitance (6.4 μF–1 day), whereas all the other membranes show lower C values, ranging from 1.5 to 3.4 μF (Figure 2B). Conversely, the resistance is lower with the reference K^+-ISM (1.1 MΩ–1 day), and it increases to values between 3.0 and 4.3 MΩ for the first set of membranes and for the second set containing PVC-COOH. The observed capacitance values are low compared to those of other SC materials with porous features [13, 62], due to the nonporous nature of the carbon ink, as reflected by the similar C obtained for the bare gold (0.66 ± 0.03 μF) and the C-ink (0.53 ± 0.12 μF). The resistance increases nearly tenfold with 25% and 50% NaPSS (9.7 and 8.6 MΩ, respectively). Unfortunately, the fully substituted NaPSS did not yield reliable CRC data, preventing further comparison with the rest of the batch, as evidenced by the contact angle (see Figure S2). After 1 week in solution, the reference K^+-ISM presents a drop of the C to 3.5 μF and NaPSS membranes show a reduced, but still higher, resistance. All the other ISMs containing PEs remain stable, indicating that after 7 days they maintained their adhesion on the SC despite their differences in composition and wettability.

Resistance is an intrinsic property of the membrane and is directly influenced by ion mobility. With the counter-charges located at the PE backbone, it may be expected to have reduced mobility compared to free KTpClPB, and therefore a higher resistance [64]. Such an observation was reported by Rosatzin et al., who used a partially sulfonated copolymer to replace borate salts [35]. Furthermore, the lower miscibility of NaPSS with lipophilic components likely induces instability in diffusion gradients due to heterogeneity in the membrane, enhancing the overall resistivity [65–68]. Such heterogeneous features can be observed in the optical images in Figure 2C. With the fully substituted PVC membrane (100% NaPSS), this resulted in uncontrolled interfacial phenomena that prevented a stable polarization curve and a reliable Ohmic potential drop from being recorded, as observed in Figure S2.

In order to elucidate the mechanical properties upon complete replacement of PVC by NaPSS various tests were performed. The Scotch tape test [51, 52], did not show any delamination for neither of the membranes that were deposited in the sensor reservoir with C-ink as the SC. While the adhesion on a reference glass slide was poor (i.e., the membranes easily delaminated), it was better for the membranes that were drop-cast onto a C-ink-coated glass slide (Figure S3A). Furthermore, the PVC-based membrane solution shows a tenfold higher viscosity compared to the one of 100% NaPSS (Figure S3B), a result that follows from the low miscibility of NaPSS with the plasticizer and the organic solvent. Finally, from rheological measurements (stress–strain curve, Figure S3C) it is possible to determine the elongation break (193 and 87%) and Young's modulus (230 and 263 Pa) for the (PVC) reference and 100% NaPSS membrane, respectively [69]. The PVC-based membrane shows a broader linear viscoelastic range (LVR) (LVR, storage modulus (G') dropping >10% of the plateau value). To conclude, both membranes maintain a gel-like behavior although the reference ISM is more flexible and less stiff than the 100% NaPSS ISM (more soft and brittle), a direct consequence of the low miscibility of the NaPSS with the plasticizer.

3.2 | Sensor Performance

To evaluate the leaching of components and degradation of the K^+-ISEs membrane, the OCP was continuously monitored in a 10 mM KCl solution for 1 week. Calibrations were performed using two sets of KCl solutions in a concentration range from 10^{-7} to 10^{-1} M. The first one was prepared in Milli-Q water, while the second one was buffered with 0.1 M of the interfering ion (Na^+). At least five replicates were prepared and measured in different batches. The linear range of the calibration curve used to calculate the slope and offset (E^0) spanned from 10^{-4} to 10^{-1} M.

The initial 24 h represent what is called the conditioning process, during which water diffuses into the membrane and the ionophore complexes with the primary ion. Simultaneously, the counter-ions, either the lipophilic salt or the PEs, may leach out the membrane, resulting in potential drift as observed in Figure 3A [8, 70]. After this process, the drift gradually declines, following a similar trend for all K^+-ISMs. An interesting aspect is

A

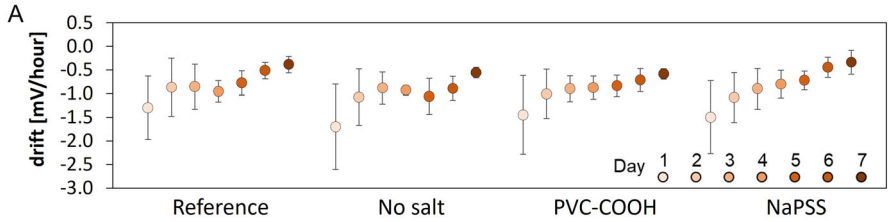

B

Membrane	Slope [mV/dec]		E^0 [mV]		Selectivity [log $K^{pot}_{K^+, Na^+}$]	
	1 day	7 days	1 day	7 days	1 day	7 days
Reference	51 ± 2	52 ± 1	543 ± 49	395 ± 25	-3.2 ± 0.2	-3.2 ± 0.3
No salt	51 ± 2	53 ± 1	540 ± 38	368 ± 30	-2.9 ± 0.4	-2.9 ± 0.3
PVC-COOH	50 ± 2	52 ± 0	534 ± 42	387 ± 10	-2.6 ± 0.3	-3.0 ± 0.2
NaPSS	51 ± 3	54 ± 3	495 ± 41	386 ± 33	-3.0 ± 0.3	-2.9 ± 0.4

FIGURE 3 | Performance of the K^+-ISM with PEs replacing the lipophilic salt over 1 week. (A) OCP drift (mV/h) in 10 mM KCl. (B) Table containing the sensitivity (slope) and offset of the calibration curve (E^0) in KCl. Selectivity coefficient ($\log K^{pot}_{K^+, Na^+}$) were determined by the FIM and a NaCl background concentration of 0.1 M. Standard deviations were obtained from minimum of five replicates.

represented by the standard deviation, which reduces as the operational time of ISE in water increases. We attribute the standard deviation trend to the conditioning of the membrane, which improves after several days of stabilization (Figure S4). After 1 week of continuous immersion in the solution, all membranes exhibited consistent performance, demonstrating slopes of ≥52 mV/dec in KCl (Figure 3B). The sub-Nernstian response may be attributed to Donnan exclusion failure together with the high level of miniaturization and the fabrication methods that differ from liquid-contact construction [71–76].

In the case of the first set of ISMs, the offset (E^0) remains unchanged regardless of the presence of PE or KTpClPB, and similar variations in E^0 were observed after 7 days (Figure 3B in KCl and Table S2 with interfering ion background). The selectivity coefficients (calculated using the FIM) range from −2.6 to −3.2 for all K^+-ISEs for the entire duration of the experiment (Figure 3B). While this selectivity is on the low side for an ionophore such as valinomycin, it does fall within the range of reported values [73, 77, 78]. Table S3 provides a comparative overview of miniaturized ISE performance reported in the literature.

Interestingly, the "no salt" ISM - prepared as a blank-displays sensitivity results comparable to those of all the other K^+-ISMs, while showing higher conditioning EMF drifts (−1.7 mV/h). The absence of the lipophilic salt, which provides counter-charges, is expected to result in very low or no sensitivity due to a failure of the Donnan exclusion effect. However, as previously reported, commercial plasticizers and PVC contain charged impurities that serve as ionic sites [59, 79]. Despite this observation, adding lipophilic salt is still a common practice to reduce membrane resistance and achieve stable potentials [10, 80, 81], and some work suggests that incorporating lipophilic ionic sites can mitigate the impact of impurities on sensor performance [82].

Figure 4A shows the drift performance of the second set of membranes. Partial substitution of PVC with PVC-COOH (25 and 50%) results in similar conditioning drifts comparable to the reference K^+-ISM composition, with values of −1.0, −1.3, and −1.4 mV/h, respectively. When PVC is fully replaced by PVC-COOH, the conditioning drift rate decreases to −0.8 mV/h. Introducing NaPSS leads to faster conditionings, with drifts of −0.4 mV/h (25% NaPSS), −0.1 mV/h (50% NaPSS), and −0.2 mV/h (100% NaPSS). This results in a sensor that requires virtually no conditioning prior to use, as the potential drift stabilizes within the first hour. This behavior may be associated with the hydrophilicity and high-charge-density of NaPSS, potentially enhancing water uptake. Throughout the rest of the experiment, all PE-containing membranes exhibited consistently low drift. We attribute this stability to two main factors: i) the use of large MW polymers to replace KTpClPB, effectively reducing membrane leaching; ii) the charges of the polymer backbone are strongly bonded to the polyanion, preventing any migration outside the membrane. Short conditioning times have been achieved in the past for SC-ISEs with PVC-based membranes and a wide variety of SC materials [70, 83, 84]. However, in the context of this work, where the difference between the tested membranes lies solely in the membrane composition. It is observed that the use of NaPSS as a membrane component resulted in reduced initial drift, and it was consistent after 7 days.

Figure 4B shows the averaged offset E^0 obtained from the calibration curves measured in KCl. The E^0 values for the reference K^+-ISM change from 543 ± 49 to 395 ± 25 mV with a drift of −148 mV throughout the experiment. Membranes containing 25%, 50%, and 100% PVC-COOH exhibit similar starting and ending E^0 values, slightly higher than those observed for the reference (all E^0 ~650 mV – day 1). Increasing the content of PVC-COOH reduces the E^0 drift (−139, −128, and −118 mV, respectively).

Introducing high-charge-density NaPSS lowers the initial E^0 value compared to the reference ISM. Keeping PVC in the membrane results in the same E^0 drift independently of the NaPSS content (−75 mV for 25% NaPSS, −70 mV for 50% NaPSS), while

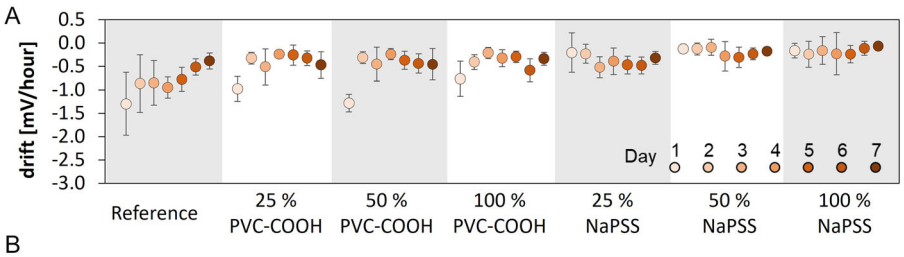

B

Membrane name	Slope [mV/dec]		E^0 [mV]		Selectivity [log $K^{pot}_{K^+, Na^+}$]	
	1 day	7 days	1 day	7 days	1 day	7 days
Reference	51 ± 2	52 ± 1	543 ± 49	395 ± 25	-3.2 ± 0.2	-3.2 ± 0.3
25 % COOH	52 ± 0	55 ± 3	647 ± 18	508 ± 28	-2.9 ± 0.2	-3.1 ± 0.1
50 % COOH	53 ± 2	53 ± 1	655 ± 23	527 ± 21	-3.0 ± 0.1	-3.0 ± 0.2
100 % COOH	53 ± 1	53 ± 1	654 ± 13	536 ± 16	-3.1 ± 0.1	-3.0 ± 0.2
25 % NaPSS	53 ± 1	54 ± 1	482 ± 18	407 ± 12	-3.3 ± 0.1	-3.1 ± 0.1
50 % NaPSS	54 ± 0	54 ± 1	482 ± 21	412 ± 15	-3.4 ± 0.1	-3.2 ± 0.1
100 % NaPSS	53 ± 1	54 ± 1	370 ± 73	317 ± 14	-3.4 ± 0.1	-3.1 ± 0.1

FIGURE 4 | Performance of the K^+-ISM with PEs replacing the lipophilic salt and PVC over 1 week. (A) OCP drift (mV/h) in 10 mM KCl (B) table containing the sensitivity (slope) and offset of the calibration curve (E^0) in KCl. Selectivity coefficients ($\log K^{pot}_{K^+, Na^+}$) were determined by the FIM and a NaCl background concentration of 0.1 M. Standard deviations were obtained from minimum of five replicates.

the three-component NaPSS membrane shows the lowest E^0 from the full set of membranes (E^0 from 370 ± 73 to 317 ± 14 (−53 mV drift)). Such behavior is consistent with the changes observed in the wettability properties. We can conclude that, despite its higher variability, the offset drift with 100% NaPSS is reduced to half compared with the use of a low-charge-density PE such as PVC-COOH.

Calibration curves (Figure S5) confirm that sensitivity was maintained after 7 days, with slopes ≥52 mV/dec in KCl (Figure 4B) and ≥51 mV/dec with 0.1 M NaCl background (Table S2). The near overlap of the two calibration curves for the 100% PE compositions confirms a low Na^+ interference in the dynamic range of 10^{-4} to 10^{-1} M KCl (Figure S6) [8]. Selectivity coefficient values obtained by the FIM range from −2.9 to −3.4 for all K^+-ISEs and were found to be constant after 1 week in solution (Figure 4B). This indicates that the valinomycin functionality is barely compromised by the reduction of the ionophore-to-counter-charge ratio, compared to the reference ISM. At higher wt% of PE in the membrane composition, a fully dissociated NaPSS would worsen the selectivity values despite the addition of an ionophore, following the Hofmeister series [46, 85]. Therefore, it could suggest a partial dissociation of the PE sulfonate groups in the membrane. Control membranes without an ionophore were prepared and assessed (Figure S7), confirming that the high concentration of NaPSS does not influence the selectivity.

The strong hydrophilic character of the PSS membrane promotes fast hydration, which might enhance the formation of a water layer at the interface between the SC and the membrane. Therefore, performing the water layer test is a necessary step for the evaluation of the membrane's drift. As illustrated in Figure 5, the sensors were sequentially monitored in 10 mM KCl, 10 mM NaCl, and 10 mM KCl. The water layer test revealed

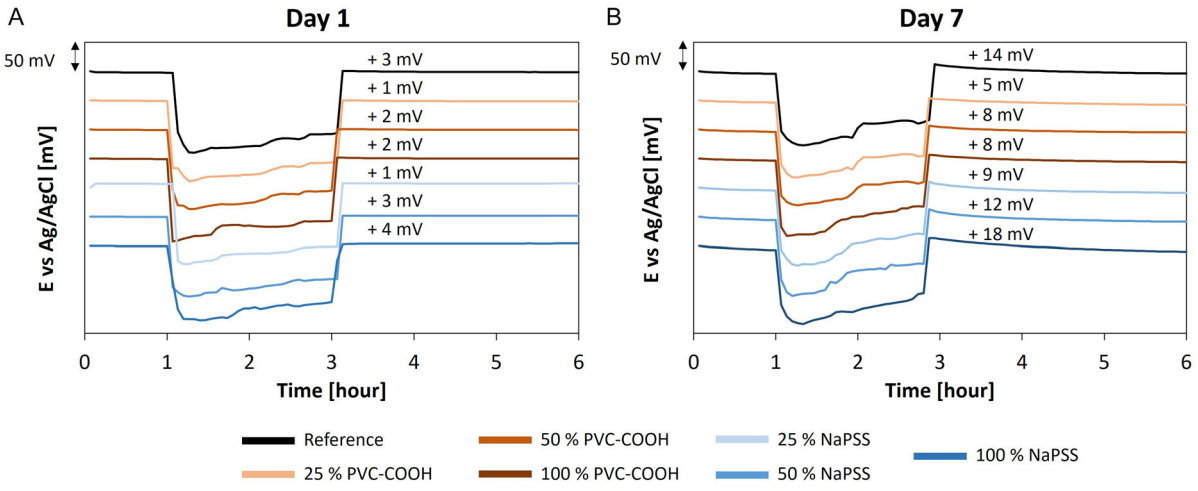

FIGURE 5 | Water layer test data of the K^+-ISM with PEs replacing the lipophilic salt and PVC after (A) 1 and (B) 7 days in solution.

that, with an increasing % of the same PE, there is a progressive increase in the EMF after the exposure to the interfering ion (Figure 5A). This trend correlates with the increase in charge density, both in terms of the transition from one PE to another and the variation in the PE percentage within the final membrane. After 1 week, the water layer trend is comparable (Figure 5B), but a larger EMF mismatch is observed. To conclude, while the increasing amount of NaPSS strongly impacts the wettability properties of the membrane, the EMF values change only with ≤4 mV after conditioning. This may indicate small differences in the water layer formation for the ISMs with different NaPSS percentages.

4 | Conclusions

The concept of using a high-charge-density PE as an alternative to the traditional matrix polymer (PVC) and ion exchangers (KTpClPB) to fabricate three-component ISMs has been explored for the first time. NaPSS was incorporated as a component for the formulation of drop-cast ISE membranes, and assessed through wetting studies, chronopotentiometry, and potentiometry.

While keeping PVC as the matrix polymer, replacing the traditionally used lipophilic borate salts with PVC-COOH, as well as NaPSS, preserved the membrane's characteristics and performance. The partial substitution of PVC (25% and 50%) by PVC-COOH had no impact on the conditioning drifts. In contrast, the use of NaPSS reduced this parameter by tenfold. The sensitivity and selectivity values of all K^+-ISEs were consistent over 7 days. The complete replacement of PVC by NaPSS induced a dramatic change in the ISM surface wettability, where the SWCA values dropped from 85° to 41°, indicating higher hydrophilicity. Despite this, the sensor performance remained unaffected, with a drift of –0.2 mV/h. This corresponds to a reduction of the drift rate by up to 80% compared to a traditional K^+-ISM composition. This feature, combined with comparable performances, makes the three-component NaPSS membrane an interesting alternative to the conventional four-component ISM for K^+ sensing. Such a change in wettability appears to have a low influence on the water layer formation at the SC–ISM interface compared to the PVC-based membrane. Further morphological investigation is required, as well as testing the effects of changing other parameters, such as the membrane cocktail solvent and the type of plasticizer.

A fast conditioning behavior is pointed out as advantageous, as it enables a more effective implementation in single-use applications such as point-of-care ISEs [71], where an initial overnight conditioning is still found to be a requirement [2]. Moreover, NaPSS offers a promising pathway to develop new ISM formulations with cheaper, commercially available compounds that are more environmentally friendly. The presence of a sulfonate group also points to the potential of chemical modifications.

Besides membrane degradation, the drift and performance of the sensor are influenced by other parameters such as the SC, the conductive substrate material, membrane thickness, and the sensor substrate. While those have not been considered for this proof-of-concept, they will need to be taken into account in further investigations. To conclude, introducing a significant percentage of highly charged polymer (NaPSS) in the ISM paves the way for future research on PEs in the membrane composition.

Author Contributions

Júlia Mestres: conceptualization, methodology, validation, formal analysis, investigation, data curation, writing–original draft, writing–review and editing, visualization. **Jayaruwan G. Gamaethiralalage**: validation, writing–review and editing. **Louis C. P. M. de Smet**: conceptualization, methodology, validation, writing–review and editing, supervision, funding acquisition, project administration. **Francesca Leonardi**: conceptualization, methodology, validation, writing–review and editing, supervision. All authors have given approval to the final version of the manuscript.

Acknowledgments

The authors acknowledge financial support from the Dutch Research Council (NWO Launchpad for Innovative Future Technology Grant, SALDIS, ENPPS.LIFT.019.034). L.C.P.M.d.S. and J.G.G. acknowledge financial support from the European Research Council (ERC Proof of Concept, PassIon, 101158035). F.L. acknowledges financial support from the Provincie Gelderland. J.M. acknowledges the technical support provided by OnePlanet Research Center. The authors thank Dr. Simon van Hurne (Wageningen University) for valuable support with the rheology data analysis.

Conflicts of Interest

The authors declare no conflicts of interest.

Data Availability Statement

The data that support the findings of this study are available from the corresponding author upon reasonable request.

References

1. M. Chandra and K. Vinod, "Ion-Selective Electrodes Based on PVC Membranes for Potentiometric Sensor Applications: A Review," *International Journal of Membrane Science and Technology* 8 (2021): 76–84.

2. Á. Molinero-Fernández, A. Casanova, Q. Wang, M. Cuartero, and G. A. Crespo, "In Vivo Transdermal Multi-Ion Monitoring with a Potentiometric Microneedle-Based Sensor Patch," *ACS Sensors* 8 (2023): 158–166.

3. D. D. Zhu, Y. R. Tan, L. W. Zheng, et al., "Microneedle-Coupled Epidermal Sensors for In-Situ-Multiplexed Ion Detection in Interstitial Fluids," *ACS Applied Materials & Interfaces* 15 (2023): 14146–14154.

4. J. Zhai, B. Luo, A. Li, H. Dong, X. Jin, and X. Wang, "Unlocking All-Solid Ion Selective Electrodes: Prospects in Crop Detection," *Sensors* 22 (2022): 5541.

5. N. Jadon, B. Hosseinzadeh, S. I. Kaya, G. Ozcelikay-Akyildiz, A. Cetinkaya, and S. A. Ozkan, "Emerging Trends of Ion-Selective Electrodes in Pharmaceutical Applications," *Electrochimica Acta* 488 (2024): 144204.

6. M. E. Cakmak, O. Özbek, K. B. Akar, and M. B. Gürdere, "Selective and Fast Potentiometric Sensors Based on Thiosemicarbazone with Low Detection Limit for the Determination of Cu2+ Ions," *Microchemical Journal* 209 (2025): 112894.

7. O. C. Altunoluk, O. Özbek, H. Akbas, and Ö. Isildak, "Highly Selective Potentiometric Detection of Arsenate Ions Based on a Newly Synthesized Protic Alkanolammonium Ionic Liquid," *Microchemical Journal* 213 (2025): 113784.

8. C. Bieg, K. Fuchsberger, and M. Stelzle, "Introduction to Polymer-Based Solid-Contact Ion-Selective Electrodes—basic Concepts, Practical Considerations, and Current Research Topics," *Analytical and Bioanalytical Chemistry* 409 (2017): 45–61.

9. K. Maksymiuk, E. Stelmach, and A. Michalska, "Unintended Changes of Ion-Selective Membranes Composition—Origin and Effect on Analytical Performance," *Membranes* 10 (2020): 266.

10. S. Yajima, K. Tohda, P. Bühlmann, and Y. Umezawa, "Donnan Exclusion Failure of Neutral Ionophore-Based Ion-Selective Electrodes Studied by Optical Second-Harmonic Generation," *Analytical Chemistry* 69 (1997): 1919–1924.

11. E. Bakker, P. Bühlmann, and E. Pretsch, "Carrier-Based Ion-Selective Electrodes and Bulk Optodes. 1. General Characteristics," *Chemical Reviews* 97 (1997): 3083–3132.

12. F. Li, J. Ye, M. Zhou, et al., "All-Solid-State Potassium-Selective Electrode Using Graphene as the Solid Contact," *The Analyst* 137 (2012): 618–623.

13. Z. Zhang and I. Papautsky, "Miniature Ion-Selective Electrodes with Mesoporous Carbon Black as Solid Contact," *Electroanalysis* 33 (2021): 2143–2151.

14. N. Lenar, R. Piech, and B. Paczosa-Bator, "Potentiometric Sensor with High Capacity Composite Composed of Ruthenium Dioxide and Poly(3,4-Ethylenedioxythiophene) Polystyrene Sulfonate," *Materials* 14 (2021): 1891.

15. R. Cánovas, S. Padrell Sánchez, M. Parrilla, M. Cuartero, and G. A. Crespo, "Cytotoxicity Study of Ionophore-Based Membranes: Toward On-Body and in Vivo Ion Sensing," *ACS Sensors* 4 (2019): 2524–2535.

16. B. Hambly, M. Guzinski, B. Pendley, and E. Lindner, "Evaluation, Pitfalls and Recommendations for the 'Water Layer Test' for Solid Contact Ion-Selective Electrodes," *Electroanalysis* 32 (2020): 781–791.

17. E. Lindner and R. E. Gyurcsányi, "Quality Control Criteria for Solid-Contact, Solvent Polymeric Membrane Ion-Selective Electrodes," *Journal of Solid State Electrochemistry* 13 (2009): 51–68.

18. Y. Qin, S. Peper, A. Radu, A. Ceresa, and E. Bakker, "Plasticizer-Free Polymer Containing a Covalently Immobilized Ca2+-Selective Ionophore for Potentiometric and Optical Sensors," *Analytical Chemistry* 75 (2003): 3038–3045.

19. K. R. Choi, X. V. Chen, J. Hu, and P. Bühlmann, "Solid-Contact pH Sensor with Covalent Attachment of Ionophores and Ionic Sites to a Poly(decyl Methacrylate) Matrix," *Analytical Chemistry* 93 (2021): 16899–16905.

20. M. Pawlak, E. Grygolowicz-Pawlak, G. A. Crespo, G. Mistlberger, and E. Bakker, "PVC-Based Ion-Selective Electrodes with Enhanced Biocompatibility by Surface Modification with 'Click' Chemistry," *Electroanalysis* 25 (2013): 1840–1846.

21. E. M. Zahran, A. New, V. Gavalas, and L. G. Bachas, "Polymeric Plasticizer Extends the Lifetime of PVC-Membrane Ion-Selective Electrodes," *The Analyst* 139 (2014): 757–763.

22. T. Wang, C. Cui, Y. Huang, et al., "Ion Selective Nano-Mesh Electrode for Long-Term Continuous Monitoring of Wastewater Quality Fabricated Using Template-Guided Membrane Immobilization," *Environmental Science: Nano* 9 (2022): 2149–2160.

23. K. R. Choi, B. K. Troudt, and P. Bühlmann, "Ion-Selective Electrodes With Sensing Membranes Covalently Attached to Both the Inert Polymer Substrate and Conductive Carbon Contact," *Angewandte Chemie International Edition* 62 (2023): e202304674.

24. G. Högg, O. Lutze, and K. Cammann, "Novel Membrane Material for Ion-Selective Field-Effect Transistors with Extended Lifetime and Improved Selectivity," *Analytica Chimica Acta* 335 (1996): 103–109.

25. A. Cao, M. Mescher, D. Bosma, J. H. Klootwijk, E. J. R. Sudhölter, and L. C. P. M. de Smet, "Ionophore-Containing Siloprene Membranes: Direct Comparison between Conventional Ion-Selective Electrodes and Silicon Nanowire-Based Field-Effect Transistors," *Analytical Chemistry* 87 (2015): 1173–1179.

26. M. Pawlak and E. Bakker, "Chemical Modification of Polymer Ion-Selective Membrane Electrode Surfaces," *Electroanalysis* 26 (2014): 1121–1131.

27. T. Satchwill and D. J. Harrison, "Synthesis and Characterization of New Polyvinylchloride Membranes for Enhanced Adhesion of Electrode Surfaces," *Journal of Electroanalytical Chemistry and Interfacial Electrochemistry* 202 (1986): 75–81.

28. V. V. Cosofret, M. Erdösy, R. P. Buck, et al., "Electroanalytical and Biocompatibility Studies on Carboxylated Poly(vinyl Chloride) Membranes for Microfabricated Array Sensors," *The Analyst* 119 (1994): 2283–2292.

29. S. C. Ma, N. A. Chaniotakis, and M. E. Meyerhoff, "Response Properties of Ion-Selective Polymeric Membrane Electrodes Prepared with Aminated and Carboxylated Poly(vinyl Chloride)," *Analytical Chemistry* 60 (1988): 2293–2299.

30. V. V. Cosofret, R. P. Buck, and M. Erdosy, "Carboxylated Poly(vinyl Chloride) as a Substrate for Ion Sensors: Effects of Native Ion Exchange on Responses," *Analytical Chemistry* 66 (1994): 3592–3599.

31. M. Pietrzak, M. Mroczkiewicz, and E. Malinowska, "Application of F-Selective Ionophores in Carboxylated or Aminated Poly(Vinyl Chloride)-Based Membranes of Ion-Selective Electrodes," *Electroanalysis* 24 (2012): 173–179.

32. J.-L. Lin and H.-Y. Hsu, "Study of Sodium Ion Selective Electrodes and Differential Structures with Anodized Indium Tin Oxide," *Sensors* 10 (2010): 1798–1809.

33. F. Yusupov, A. Kucharov, G. Baymatova, B. Shukurullayev, and R. Yuldashev, "Development and Study of Adsorption Properties of a New Sulfur Polyvinyl Chloride Cation Exchanger for Water Treatment," *IOP Conference Series: Earth and Environmental Science* 1231 (2023): 012027.

34. J. T. S. Allan, L. E. Prest, and E. B. Easton, "The Sulfonation of Polyvinyl Chloride: Synthesis and Characterization for Proton Conducting Membrane Applications," *Journal of Membrane Science* 489 (2015): 175–182.

35. T. Rosatzin, E. Bakker, K. Suzuki, and W. Simon, "Lipophilic and Immobilized Anionic Additives in Solvent Polymeric Membranes of Cation-Selective Chemical Sensors," *Analytica Chimica Acta* 280 (1993): 197–208.

36. M. Guzinski, J. M. Jarvis, F. Perez, et al., "PEDOT(PSS) as Solid Contact for Ion-Selective Electrodes: The Influence of the PEDOT(PSS) Film Thickness on the Equilibration Times," *Analytical Chemistry* 89 (2017): 3508–3516.

37. M. Mir, R. Lugo, I. Tahirbegi, and J. Samitier, "Miniaturizable Ion-Selective Arrays Based on Highly Stable Polymer Membranes for Biomedical Applications," *Sensors* 14 (2014): 11844–11854.

38. E. Zdrachek and E. Bakker, "Potentiometric Sensing," *Analytical Chemistry* 91 (2019): 2–26.

39. T. Momma, S. Komaba, M. Yamamoto, T. Osaka, and S. Yamauchi, "All-Solid-State Potassium-Selective Electrode Using Double-Layer Film of Polypyrrole/Polyanion Composite and Plasticized Poly(vinyl Chloride) Containing Valinomycin," *Sensors and Actuators B: Chemical* 25 (1995): 724–728.

40. R. Sharma, M. Geranpayehvaghei, F. Ejeian, A. Razmjou, and M. Asadnia, "Recent Advances in Polymeric Nanostructured Ion Selective Membranes for Biomedical Applications," *Talanta* 235 (2021): 122815.

41. A. A. Stekolshchikova, A. V. Radaev, O. Y. Orlova, K. G. Nikolaev, and E. V. Skorb, "Thin and Flexible Ion Sensors Based on Polyelectrolyte Multilayers Assembled onto the Carbon Adhesive Tape," *ACS Omega* 4 (2019): 15421–15427.

42. L. V. Pershina, A. R. Grabeklis, L. N. Isankina, E. V. Skorb, and K. G. Nikolaev, "Determination of Sodium and Potassium Ions in Patients with SARS-Cov-2 Disease by Ion-Selective Electrodes Based on Polyelectrolyte Complexes as a Pseudo-Liquid Contact Phase," *RSC Advances* 11 (2021): 36215–36221.

43. C.-A. Ghiorghita and M. Mihai, "Recent Developments in Layer-by-Layer Assembled Systems Application in Water Purification," *Chemosphere* 270 (2021): 129477.

44. S. Sahin, J. E. Dykstra, H. Zuilhof, R. L. Zornitta, and L. C. P. M. de Smet, "Modification of Cation-Exchange Membranes with Polyelectrolyte Multilayers to Tune Ion Selectivity in Capacitive Deionization," *ACS Applied Materials & Interfaces* 12 (2020): 34746–34754.

45. J. G. Gamaethiralalage, K. Singh, S. Sahin, et al., "Recent Advances in Ion Selectivity with Capacitive Deionization," *Energy & Environmental Science* 14 (2021): 1095–1120.

46. E. Grygolowicz-Pawlak, G. A. Crespo, M. Ghahraman Afshar, G. Mistlberger, and E. Bakker, "Potentiometric Sensors with Ion-Exchange Donnan Exclusion Membranes," *Analytical Chemistry* 85 (2013): 6208–6212.

47. S. Krivačić, A. Speck, P. Kassal, and E. Bakker, "Towards Mass-Production of Ion-Selective Electrodes by Spotting: Optimization of Membrane Composition and Real-Time Tracking of Membrane Drying," *Sensors and Actuators B: Chemical* 423 (2025): 136759.

48. M. Rostampour, B. Bailey, C. Autrey, et al., "Single-Step Integration of Poly(3-Octylthiophene) and Single-Walled Carbon Nanotubes for Highly Reproducible Paper-Based Ion-Selective Electrodes," *Analytical Chemistry* 93 (2021): 1271–1276.

49. D. Wang, W. Zhang, J. Wang, X. Li, and Y. Liu, "A High-Performance, All-Solid-State Na^+ Selective Sensor Printed with Eco-Friendly Conductive Ink," *RSC Advances* 13 (2023): 16610–16618.

50. M. Rostampour, D. J. Lawrence, Z. Hamid, J. Darensbourg, P. Calvo-Marzal, and K. Y. Chumbimuni-Torres, "Highly Reproducible Flexible Ion-Selective Electrodes for the Detection of Sodium and Potassium in Artificial Sweat," *Electroanalysis* 35 (2023): e202200121.

51. X. V. Chen and P. Bühlmann, "Ion-Selective Potentiometric Sensors with Silicone Sensing Membranes: A Review," *Current Opinion in Electrochemistry* 32 (2022): 100896.

52. Y. Fan, X. Qian, X. Wang, et al., "Enhancing Long-Term Accuracy and Durability of Wastewater Monitoring Using Electrosprayed Ultra-Thin Solid-State Ion Selective Membrane Sensors," *Journal of Membrane Science* 643 (2022): 119997.

53. F. Criscuolo, M. I. N. Hanitra, I. Taurino, S. Carrara, and G. De Micheli, "All-Solid-State Ion-Selective Electrodes: A Tutorial for Correct Practice," *IEEE Sensors Journal* 21 (2021): 22143–22154.

54. J. Bobacka, A. Ivaska, and A. Lewenstam, "Potentiometric Ion Sensors," *Chemical Reviews* 108 (2008): 329–351.

55. M. Krzywinski and N. Altman, "Visualizing Samples with Box Plots," *Nature Methods* 11 (2014): 119–120.

56. Y. Umezawa, K. Umezawa, and H. Sato, "Selectivity coefficients for ion-selective electrodes: Recommended methods for reporting KA,Bpot values (Technical Report)," *Pure and Applied Chemistry* 67 (1995): 507–518.

57. M. Monika, S. K. Mahto, S. Das, et al., "Chemical Modification of Poly(vinyl Chloride) for Blood and Cellular Biocompatibility," *RSC Advances* 5 (2015): 45231–45238.

58. E. Stelmach, J. Kalisz, B. Wagner, K. Maksymiuk, and A. Michalska, "Nanofiber Ion-Selective Membrane-Coated Carbon Paper All-Solid-State Sensors: One Stone, Two Birds," *Analytical Chemistry* 96 (2024): 3253–3258.

59. Q. Ye, G. Horvai, A. Tóth, I. Bertóti, M. Botreau, and T. M. Duc, "Studies of Ion-Selective Solvent Polymeric Membranes by X-Ray Photoelectron Spectroscopy and Time-of-Flight Static Secondary Ion Mass Spectroscopy," *Analytical Chemistry* 70 (1998): 4241–4246.

60. M. Krasowska, J. Zawala, and K. Malysa, "Air at Hydrophobic Surfaces and Kinetics of Three Phase Contact Formation," *Advances in Colloid and Interface Science* 147–148 (2009): 155–169.

61. A. V. Kalinichev, E. V. Solovyeva, A. R. Ivanova, G. A. Khripoun, and K. N. Mikhelson, "Non-Constancy of the Bulk Resistance of Ionophore-Based Cd2+-Selective Electrode: A Correlation with the Water Uptake by the Electrode Membrane," *Electrochimica Acta* 334 (2020): 135541.

62. E. Zdrachek and E. Bakker, "Ion-to-Electron Capacitance of Single-Walled Carbon Nanotube Layers before and after Ion-Selective Membrane Deposition," *Microchimica Acta* 188 (2021): 149.

63. J. Hu, A. Stein, and P. Bühlmann, "Rational Design of All-Solid-State Ion-Selective Electrodes and Reference Electrodes," *TrAC, Trends in Analytical Chemistry* 76 (2016): 102–114.

64. R. J. W. Lugtenberg, R. J. M. Egberink, A. van den Berg, J. F. J. Engbersen, and D. N. Reinhoudt, "The Effects of Covalent Binding of the Electroactive Components in Durable CHEMFET Membranes—impedance Spectroscopy and Ion Sensitivity Studies," *Journal of Electroanalytical Chemistry* 452 (1998): 69–86.

65. Y. Tsujimura, M. Yokoyama, and K. Kimura, "Practical Applicability of Silicone Rubber Membrane Sodium-Selective Electrode Based on Oligosiloxane-Modified Calix[4]arene Neutral Carrier," *Analytical Chemistry* 67 (1995): 2401–2404.

66. J. Choi, "Pore Size Characterization of Cation-Exchange Membranes by Chronopotentiometry Using Homologous Amine Ions," *Journal of Membrane Science* 191 (2001): 225–236.

67. H.-J. Lee, M.-K. Hong, S.-D. Han, and S.-H. Moon, "Influence of the Heterogeneous Structure on the Electrochemical Properties of Anion Exchange Membranes," *Journal of Membrane Science* 320 (2008): 549–555.

68. Z. Stojek, "The Electrical Double Layer and Its Structure," in, Electroanalytical Methods Guide to Experiments and Applications, ed. F. Scholz (Springer Berlin Heidelberg, 2010), 3–9.

69. Y. Li, X. Feng, L. Zhu, et al., "High Performance Fiber-Constrained Plasticized PVC Gel Actuators for Soft Robotics," *Sensors and Actuators B: Chemical* 393 (2023): 134177.

70. Y. H. Cheong, L. Ge, and G. Lisak, "Highly Reproducible Solid Contact Ion Selective Electrodes: Emerging Opportunities for Potentiometry–A Review," *Analytica Chimica Acta* 1162 (2021): 338304.

71. E. J. Herrero and P. Bühlmann, "Challenges and Opportunities in the Development of Planar Potentiometric Sensors for Point-of-Care Analysis," *TrAC, Trends in Analytical Chemistry* 181 (2024): 118002.

72. V. A. T. Dam and M. Zevenbergen, "*Multi-Ion Sensor Chip for Healthcare Applications*," in 22nd International Conference on Solid-State Sensors, Actuators and Microsystems (Transducers) (IEEE, 2023), 1168–1171.

73. E. Jarosińska, J. Wojnowska, M. Durka, M. Podrażka, and E. Witkowska Nery, "Low-Cost, Syringe Based Ion-Selective Electrodes for the Evaluation of Potassium in Food Products and Pharmaceuticals," *Electrochimica Acta* 508 (2024): 145209.

74. H. J. Park, J.-M. Jeong, J. H. Yoon, et al., "Preparation of Ultrathin Defect-Free Graphene Sheets from Graphite via Fluidic Delamination for Solid-Contact Ion-to-Electron Transducers in Potentiometric Sensors," *Journal of Colloid and Interface Science* 560 (2020): 817–824.

75. J. H. Yoon, H. J. Park, S. H. Park, K. G. Lee, and B. G. Choi, "Electrochemical Characterization of Reduced Graphene Oxide as an Ion-to-Electron Transducer and Application of Screen-Printed All-Solid-State Potassium Ion Sensors," *Carbon Letters* 30 (2020): 73–80.

76. S. O. Mirabootalebi and Y. Liu, "Recent Advances in Nanomaterial-Based Solid-Contact Ion-Selective Electrodes," *The Analyst* 149 (2024): 3694–3710.

77. H. Liu, Z. Gu, Q. Zhao, et al., "Printed Circuit Board Integrated Wearable Ion-Selective Electrode with Potential Treatment for Highly Repeatable Sweat Monitoring," *Sensors and Actuators B: Chemical* 355 (2022): 131102.

78. M. P. S. Mousavi, A. Ainla, E. K. W. Tan, et al., "Ion Sensing with Thread-Based Potentiometric Electrodes," *Lab on a Chip* 18 (2018): 2279–2290.

79. V. Keresten, F. Lazarev, and K. Mikhelson, "Transfer of Sodium Ion across Interface between Na+-Selective Electrode Membrane and Aqueous Electrolyte Solution: Can We Use Nernst Equation If Current Flows through Electrode?," *Membranes* 14 (2024): 74.

80. P. Bühlmann, S. Yajima, K. Tohda, and Y. Umezawa, "EMF Response of Neutral-Carrier Based Ion-Sensitive Field Effect Transistors with Membranes Free of Ionic Sites," *Electrochimica Acta* 40 (1995): 3021–3027.

81. A. Seki, K. Motoya, S. Watanabe, and I. Kubo, "Novel Sensors for Potassium, Calcium and Magnesium Ions Based on a Silicon Transducer as a Light-Addressable Potentiometric Sensor," *Analytica Chimica Acta* 382 (1999): 131–136.

82. M. Nägele and E. Pretsch, "New Method for Determining the Concentration of Ionic Impurities in Solvent Polymeric Membranes," *Mikrochimica Acta* 121 (1995): 269–279.

83. M. Guzinski, J. M. Jarvis, B. D. Pendley, and E. Lindner, "Equilibration Time of Solid Contact Ion-Selective Electrodes," *Analytical Chemistry* 87 (2015): 6654–6659.

84. C. R. Rousseau and P. Bühlmann, "Calibration-Free Potentiometric Sensing with Solid-Contact Ion-Selective Electrodes," *TrAC, Trends in Analytical Chemistry* 140 (2021): 116277.

85. K. Wojciechowski, "Hydration Energy or Hydration Force? Origin of Ion-Specificity in Ion Selective Electrodes," *Current Opinion in Colloid & Interface Science* 16 (2011): 601–606.

Supporting Information

Additional supporting information can be found online in the Supporting Information section. **Supporting Fig. S1**: Chemical structure of valinomycin. **Supporting Fig. S2**: Representative data of CRC curves. The unstable potential drift for 100% NaPSS K^+-ISM made it infeasible to calculate capacitance and resistance parameters. **Supporting Fig. S3**: Overview of the mechanical properties of the reference PVC-based membrane and the 100% NaPSS membrane and their solutions. (A) Scotch tape adhesion tests on – from left to right – the sensor reservoir, a glass slide, and on the solid contact (Cink), (B) viscosity data, and (C) stress-strain curve (left) and shear modulus-strain in log-log (right). The closed circles correspond to the storage modulus (G′) whereas the open ones the loss modulus (G''). **Supporting Fig. S4**: Normalized OCP data of the first set of K^+-ISM (n = 5) recorded during the conditioning and the final 24 hours. **Supporting Fig. S5**: Calibration curves (in KCl) of one representative replicate from the second set of K+-ISMs, after (A) one and (B) seven days. Linear range from 10^{-4} to 10^{-1} M KCl. **Supporting Fig. S6**: Calibration curves of one representative replicate (in KCl (•) and with 0.1 M NaCl interfering ion (▲)) of the reference, 100% PVC-COOH, and 100% NaPSS K^+-ISMs (from left to right). **Supporting Fig. S7**: Calibration curves with the presence of interfering ion (0.1 M NaCl) after the first conditioning of the reference, 25% NaPSS, 50% NaPSS, and 100% NaPSS K^+-ISM (from left to right). With (•) and without ionophore (▲). **Supporting Table S1**: Composition of all potassium ion-selective membranes in weight% (mol%). **Supporting Table S2**: Sensitivity (slope of the calibration curve) and offset (E^0) obtained from calibration curves with 0.1 M NaCl background electrolyte. Standard deviation obtained from a minimum of five replicates measured in different batches. **Supporting Table S3**: Brief literature overview of the K^+-ISE performance in miniaturized solid contact ISEs.